Prospective intra-individual blinded comparison of [^{18}F]PSMA-1007 and [^{68}Ga]Ga-PSMA-11 PET/CT imaging in patients with confirmed prostate cancer

David A Pattison (david.pattison@health.qld.gov.au)
Royal Brisbane and Women's Hospital https://orcid.org/0000-0001-9718-5598

Maciej Debowski
Royal Brisbane and Women's Hospital

Brook Gulhane
Royal Brisbane and Women's Hospital

Evyn G. Arnfield
Royal Brisbane and Women's Hospital

Anita M. Pelecanos
QIMR Berghofer Medical Research Institute

Peter L. Garcia
Royal Brisbane and Women's Hospital

Melissa J. Latter
Royal Brisbane and Women's Hospital

Charles Y. Lin
Royal Brisbane and Women's Hospital

Matthew J. Roberts
Royal Brisbane and Women's Hospital

Stuart C. Ramsay
Royal Brisbane and Women's Hospital

Paul A. Thomas
Royal Brisbane and Women's Hospital

Research Article

Keywords: [18F]PSMA-1007, [68Ga]Ga-PSMA-11, prostate cancer, PET/CT

Posted Date: April 27th, 2021

DOI: https://doi.org/10.21203/rs.3.rs-455041/v1

Version of Record: A version of this preprint was published at European Journal of Nuclear Medicine and Molecular Imaging on August 12th, 2021. See the published version at https://doi.org/10.1007/s00259-021-05520-y.

Abstract

Introduction

[^{18}F]PSMA-1007 has potential advantages over [^{68}Ga]Ga-PSMA-11, although limited prospective data evaluating diagnostic performance exist. The aims of this study are to describe the concordance of [^{18}FPSMA-1007 and [^{68}Ga]Ga-PSMA-11 for TNM with American Joint Committee on Cancer (AJCC) prognostic stage, and assess differences in tracer uptake.

Methods

Fifty men (mean age 71.8) were imaged with [^{68}Ga]Ga-PSMA-11 and [^{18}F]PSMA-1007 < 4 weeks apart. Images were independently reported according to TNM by two experienced nuclear medicine specialists blinded to the other scan and prior imaging. Discordant results were resolved by a third independent nuclear medicine specialist. Quantitative analysis of lesion uptake and physiologic tissue for each tracer was performed by one experienced reader.

Results

Scan indications were initial staging (n = 12), biochemical recurrence (n = 27) and metastatic disease evaluation (n = 11). Most patients had ISUP grade group 3 or higher. Median PSA value was 2.7 ng/ml (IQR 0.7–12.0) and a minority of patients (28%) were currently treated with androgen deprivation therapy. [^{18}F]PSMA-1007 uptake was significantly higher than [^{68}Ga]Ga-PSMA-11 in local recurrence, nodal and distant metastases, and most physiologic sites except for urinary bladder which was significantly lower. [^{18}F]PSMA-1007 upstaged local prostate staging in 5/17 patients, local recurrence in 3/33 patients, regional nodal disease in 3/50 patients and 1 distant metastasis (bladder). [^{68}Ga]Ga-PSMA-11 upstaged regional nodal disease in 1/50 patients and distant metastasis in one patient (right adrenal). Overall AJCC prognostic stage was concordant in 46/50 (92%) patients, with two patients upstaged for both [^{18}F]PSMA-1007 and [^{68}Ga]Ga-PSMA-11. [^{18}F]PSMA-1007 had more equivocal results (one regional node; six equivocal bone lesions, one of which was subsequently confirmed metastatic) than [^{68}Ga]Ga-PSMA-11 (one equivocal local recurrence).

Conclusion

Overall AJCC prognostic stage was similar (92%) between [^{18}F]PSMA-1007 and [^{68}Ga]Ga-PSMA-11. [^{18}F]PSMA-1007 demonstrates higher uptake within involved nodes and distant metastases, and most physiologic sites except urinary bladder which aided [^{18}F]PSMA-1007 local staging of the prostate primary / local recurrence and regional nodal disease adjacent ureters. However [^{18}F]PSMA-1007 liver uptake obscured a solitary right adrenal metastasis, and more equivocal bone lesions were identified.

Introduction:

Prostate cancer is responsible for an estimated 366 000 deaths annually worldwide and is the most commonly diagnosed male cancer in Australia(1). The early detection and accurate staging of prostate cancer is crucial for the implementation of appropriate therapies. Prostate specific membrane antigen (PSMA) is a type II transmembrane glycoprotein present on prostate epithelial cells that is significantly over-expressed in prostate malignancy, correlating with androgen independence, metastasis, disease progression and Gleason score(2, 3). A number of PSMA-binding radiopharmaceuticals have been developed, particularly the PET tracers [^{68}Ga]Ga-PSMA-11, [^{18}F]PSMA-DCFPyL and [^{18}F]PSMA-1007. The first of these, [^{68}Ga]Ga-PSMA-11 rapidly became commonly used and suggested as the new standard of care for staging(4), re-staging at biochemical recurrence(5) and theranostic approach to prostate malignancy(6) given its superior sensitivity and specificity, interobserver reliability(7) and correlation with [^{177}Lu]Lu-PSMA-617 tumour dosimetry and treatment outcomes(8).

There are several limitations to [^{68}Ga]Ga-PSMA-11 restricting more widespread adoption and use. Gallium-68's (^{68}Ga) short half-life of 68 minutes limits tracer usage to large centres to justify the cost of an on-site generator to produce the radiotracer. Each production run is labour intensive and produces only enough activity for approximately three patient doses. Urinary excretion of [^{68}Ga]Ga-PSMA-11 radiotracer may also limit identification of small volume disease adjacent to the ureters, bladder and prostatic urethra(9) requiring use of contrast or diuretics and their associated side effects in some centres. Intense urinary uptake in the bladder and kidneys may also lead to a flair/halo artefact, limiting the detection of disease in adjacent pelvic tissues(10). Furthermore, incorrect ^{68}Ga dose calibration may impact upon quantitative accuracy(11).

More recently developed [^{18}F]PSMA-1007 and [^{18}F]PSMA-DCFPyL are labelled with fluorine-18 (^{18}F) which has a longer radioactive half-life of 110 minutes, enables central manufacture for distribution to satellite centres and more efficient labour manufacture costs. ^{18}F also exhibits a lower positron energy (0.65 MeV) when compared with ^{68}Ga (1.9 MeV), theoretically yielding higher spatial resolution. Furthermore, [^{18}F]PSMA-1007 biodistribution studies demonstrate reduced accumulation in the bladder than seen with [^{68}Ga]Ga-PSMA-11 or 18F-DCFPyL offering theoretical advantages for locoregional staging adjacent the urinary bladder and ureters. Early small retrospective studies demonstrate similar outcomes for evaluation of staging (12, 13), biochemical recurrence(14, 15) and theranostic applications(16). However, a retrospective matched-pair comparison of [^{68}Ga]Ga-PSMA-11 and [^{18}F]PSMA-1007 PET/CT demonstrated higher numbers of avid lesions attributed to a benign origin(17). A small (n=16) prospective comparison between the two tracers with histopathologic correlation was restricted to intraprostatic assessment(18), and another assessed the role of [^{18}F]PSMA-1007 in selected patients with equivocal or oligometastatic scans using a variety of renally excreted tracers(19). The aim of this study was to conduct a comprehensive, prospective intra-individual comparison of [^{18}F]PSMA-1007 and [^{68}Ga]Ga-PSMA-11 in a broad cohort of patients to evaluate physiologic biodistribution and accuracy for staging, biochemical recurrence and metastatic disease.

Materials And Methods:

The institutional review board of the Royal Brisbane and Women's Hospital approved this prospective, single-centre study (HREC/17/QRBW/686) and all patients provided written informed consent. The study was conducted according to local regulations and laws, the ethical principles in the Declaration of Helsinki and the principles of Good Clinical Practice. The study was registered with the Australian New Zealand Clinical Trials Registry (ACTRN12618000665235).

Patient Selection

From May to December 2018, 50 men were recruited according to the following eligibility criteria: (a) aged 18 years or older, (b) provided informed consent and able to comply with the study procedures, and (c) fit the criteria for one of the following scan indication categories: primary staging, biochemical recurrence (post-prostatectomy or post-radiotherapy) or restaging of distant metastatic disease. Primary staging was defined as newly diagnosed, untreated, prostate cancer based on biopsy proven intermediate-high risk adenocarcinoma Gleason grade group 3,4 or 5 and/or prostate specific antigen (PSA) greater than 20 ng/mL and/or clinical stage T3 or greater. Biochemical recurrence was defined in the post-prostatectomy setting as PSA 0.2 ng/mL or greater above the nadir following prostatectomy (R0- or R1- resection), and post-radiotherapy as PSA increase of 2 ng/mL above the lowest recorded PSA value following organ-preserving local treatment (external beam radiotherapy or brachytherapy). Metastatic disease was defined as known metastatic prostate cancer diagnosed by at least one of [^{68}Ga]Ga-PSMA-11, whole body bone scan, CT or MRI imaging or histopathologic confirmation of prostate cancer metastasis. Exclusion criteria was significant comorbidity that would limit compliance with the study protocol.

Radiotracer Synthesis

[^{68}Ga]Ga-PSMA-11 (Scintomics GRP platform) and [^{18}F]PSMA-1007 (GE FASTlab or MX Tracerlab platforms) were manufactured on site using a kit-based approach on automated platforms, with comprehensive quality control testing of each batch to monograph standards for other Ga-68 and F-18 radiopharmaceuticals respectively (pH, chemical and radiochemical purity, radionuclide identity and purity, residual solvents, sterilising filter integrity, endotoxin and sterility). Product radiochemical purity was measured by high performance liquid chromatography (HPLC) with a pre-defined acceptance criterion of >91% [^{68}Ga]Ga-PSMA-11 and >95% [^{18}F]PSMA-1007.

Image Acquisition

All patients underwent PET/CT imaging with [^{68}Ga]Ga-PSMA-11, followed by [^{18}F]PSMA-1007 within 4 weeks. Fasting was required for four hours prior to the [^{18}F]PSMA-1007 scan but there was no fasting requirement for [^{68}Ga]Ga-PSMA-11. Patients were administered either 100-150 MBq of [^{68}Ga]Ga-PSMA-11 45-60 minutes prior to imaging or 250MBq of [^{18}F]PSMA-1007 120-180 minutes prior to imaging. All patients were asked to drink approximately 500mL of water after tracer administration and voided immediately prior to the scan. Iodinated contrast was not used. All scanning parameters for [^{68}Ga]Ga-PSMA-11 and [^{18}F]PSMA-1007 scans were identical. Free breathing PET scans from skull vertex to mid-thigh were acquired using Siemens mCT Biograph PET/CT Scanners (Siemens Healthineers, Germany). Low Dose CT acquisition

was performed using automatic current modulation and 120kVp with image reconstruction to a slice thickness of 3mm. CT attenuation corrected PET images were reconstructed using an iterative algorithm with Time of Flight, Point Spread Function, Scatter and Random correction (Ultra HD), producing PET images with a matrix size of 200x200, pixel size of 4mm, slice thickness of 3mm and with a post reconstruction Gaussian filter of 5mm. Time per bed was 4 minutes over the pelvis, followed by 2.5 minutes per bed for the remainder of the scan range. The same reconstruction parameters were used for both radiotracers.

Image Analysis

Each scan was de-identified and independently reported by two Nuclear Medicine specialists experienced in the interpretation of PSMA PET studies. Reporting specialists were provided with a brief clinical history including radiotracer, indication, age, PSA, Gleason score and prior treatment and were blinded to other imaging reports. A standardised TNM reporting template according to the American Joint Committee on Cancer (AJCC) prognostic stage groups was used(20). Any discordant scan results underwent blinded evaluation by a third reader. Images were reviewed on a computer assisted reading application (Syngo.via, version VB30, Siemens Healthineers) enabling the review of PET, CT and fused imaging data in axial, sagittal and coronal planes. Maximum standardized uptake value (SUVmax) was recorded as it is considered operator-independent and suitable for small lesions. Known pitfalls in reporting of PSMA-ligand PET studies were considered. Scans were reported out of chronological order, with at least a six-week delay between reporting the complementary scans from the same patient (ie [^{68}Ga]Ga-PSMA-11 and [^{18}F]PSMA-1007 PET/CT were reported independently). Separately, comparative quantitative analysis of uptake within lesions and physiologic tissue for each tracer was performed by one experienced reader. SUVmax was used for small lesions (prostate primary, and up to 3 most avid nodal and distant metastases per patient; and left sided stellate / coeliac / sacral ganglia, left parotid gland and left inguinal node) and SUVmean using a standardised 1cm^3 sphere for larger physiologic organs (urinary bladder, liver and spleen). Clinical follow-up was performed for discordant findings and where possible was resolved by a multidisciplinary panel considering histopathology, appropriate additional imaging modality and/or PSA response in the appropriate clinical context (see Supplementary table).

Statistical Analysis

STATA 15 was used for analysis. Data were presented as mean and standard deviation (SD), median and interquartile range (IQR) or frequency and percent as appropriate. For SUVmean and SUVmax, differences between [^{18}F]PSMA-1007 and [^{68}Ga]Ga-PSMA-11 paired measurements were examined using paired t-tests. Alternatively a Wilcoxon signed rank test was used if the assumptions of the paired t-test did not hold. Statistical significance was defined as a p-value less than 0.05 (two-sided).

Results:

The mean age of the 50 men participating in the study was 71.8 years (SD 6.7). The indication for [^{18}F]PSMA-1007 PET/CT scans was initial staging (n=12), biochemical recurrence (n=27) and metastatic

disease evaluation (n=11). The majority of patient disease was International Society of Urological Pathology (ISUP) grade group 3 or higher. Median PSA value for staging, restaging and metastatic cohorts was 12ng/ml, 0.8ng/ml and 9.7ng/ml respectively. A minority of patients were treated with androgen deprivation therapy (28%) at the time of imaging. Patient characteristics are summarised in Table 1.

Significantly higher uptake at most sites of disease and physiologic organs (with the exception of bladder activity which was significantly lower) was observed for [^{18}F]PSMA-1007 compared to [^{68}Ga]Ga-PSMA-11 (Table 2). The largest difference in SUVmax at disease sites was noted for local recurrence and nodal metastases. The absolute difference (although statistically significant) for bone metastases was relatively small, and too few visceral/adrenal metastases were identified for meaningful analysis. Similarly, [^{18}F]PSMA-1007 demonstrated a significantly higher SUVmax within physiologic organs potentially confounding nodal assessment (eg. benign inguinal node, stellate / coeliac / sacral ganglia and parotid gland) and distant metastases (eg. liver, spleen). In contrast, bladder SUVmean was significantly lower with [^{18}F]PSMA-1007 than [^{68}Ga]Ga-PSMA-11, relevant for detection of lesions adjacent the bladder and ureters. Background bone marrow avidity was assessed from a region of interest in the L2 vertebral body. [^{18}F]PSMA-1007 had significantly higher bone marrow avidity (mean SUVmean of 1.5 (SD 0.5) vs 0.8 (SD 0.4), $p < 0.001$).

Local (T) staging concordance

Local (T) staging was assessed in 17 cases (12 staging and five metastatic cases with untreated primary), classified as PSMA PET stage T1/2 (intraprostatic uptake), T3a (extracapsular uptake), T3b (seminal vesicle invasion) or T4 (local invasion, including bladder & rectum). Findings were concordant in 12 cases, and in five cases [^{18}F]PSMA-1007 scans resulted in a higher local stage, particularly identifying bladder wall invasion in three cases not apparent on [^{68}Ga]Ga-PSMA-11 (see Table 3a and Figure 1). Follow-up data confirmed three of the additional / discordant findings identified with [^{18}F]PSMA-1007 were correct. The fourth case was reported T1/2 on [^{68}Ga]Ga-PSMA-11, T3b on [^{18}F]PSMA-1007, but histopathology confirmed T3a disease. There was no relevant follow-up on the fifth discordant case. These additional findings did not impact the overall stage group classification as these cases also had nodal or distant metastasis.

Local recurrence concordance

Local recurrence was assessed in 33 cases after treatment of primary prostate cancer, classified as nil, equivocal and local recurrence with or without invasion of adjacent structures (see Table 3b). Findings were concordant in 30 cases, with [^{18}F]PSMA-1007 upstaging in three cases (identifying local recurrence in two cases; one of which was equivocal on [^{68}Ga]Ga-PSMA-11 and the other had local recurrence with invasion of bladder). Follow-up data suggests one discordant case of local recurrence with invasion identified by [^{18}F]PSMA-1007 was correct, but that one case of local recurrence (equivocal on [^{68}Ga]Ga-PSMA-11) was likely false positive.

Nodal staging concordance

Fourteen cases were concordantly staged as regional node positive (see Table 3c). [^{18}F]PSMA-1007 upstaged three cases to N1 (due to proximity to ureter, see Figure 2), and in one case identified an equivocal node (classified N0 on [^{68}Ga]Ga-PSMA-11). [^{68}Ga]Ga-PSMA-11 upstaged one patient to N1 (due to focal avidity). Available follow-up confirms that an equivocal node (NE) identified on [^{18}F]PSMA-1007 was likely reactive, and two cases of discordant [^{18}F]PSMA-1007 avid nodal disease (N1) were confirmed.

Distant metastasis staging

Non-regional nodes (M1a)

Non-regional nodes (M1a) were concordantly identified in three cases (see Table 3d).

Bone (M1b)

Bone metastases were identified in 13 cases (see Table 3e). Equivocal bone lesions were identified on [^{18}F]PSMA-1007 in six patients which were not appreciable on [^{68}Ga]Ga-PSMA-11. These lesions were in ribs (n=3), clavicle (n=1), sternum (n=1) and vertebra (n=1), and were less avid than definite bone metastases. They were significantly more avid on [^{18}F]PSMA-1007 with a median SUVmax of 6.2 (IQR 5.3 – 7.9) vs 2.4 (IQR 1.5 – 3) for [^{68}Ga]Ga-PSMA-11 ($p = 0.028$). Equivocal lesions were considered M0 for the purposes of overall stage grouping. During follow-up, one patient developed definite bone metastasis at this site (T11 vertebral endplate) after 13 months (see Figure 3), whilst additional investigations in the remaining five patients confirmed a benign aetiology.

Other sites (M1c)

One patient had concordant adrenal metastasis identified ([^{18}F]PSMA-1007 SUVmax 40.4, [^{68}Ga]Ga-PSMA-11 SUVmax 36.2). One patient had a discordant bladder metastasis identified on [^{18}F]PSMA-1007 (discrete intense focal uptake on contralateral side of bladder in a patient with very extensive osseous metastatic disease) not appreciable on [^{68}Ga]Ga-PSMA-11 due to intense bladder radiourine activity (see Figure 4), and a solitary adrenal metastasis. One patient had discordant adrenal metastasis identified on [^{68}Ga]Ga-PSMA-11 (SUVmax 17.8) but not identified on [^{18}F]PSMA-1007 (SUVmax 20.6) due to adjacent similarly intense liver activity (see Figure 5). It was prospectively identified by one of the three nuclear medicine specialists, identified on retrospective review and was clinically known at time of referral (previously reported on diagnostic CT scan).

Overall AJCC prognostic stage group

The AJCC prognostic stage group was concordant in the majority of cases (46/50 patients, 92%) with discordance observed for four patients (see Table 3f). Three discordances were due to identification of regional lymph nodes ([^{18}F]PSMA-1007 upstaged in two cases [confirmed N1], [^{68}Ga]Ga-PSMA-11 upstaged

in one case [no follow-up available]). One discordance was due to histopathologically confirmed right adrenal metastasis adjacent to intense liver activity on [^{18}F]PSMA-1007.

Discussion:

This is the largest prospective intra-individual comparative study of [^{18}F]PSMA-1007 vs [^{68}Ga]Ga-PSMA-11 for prostate cancer staging, evaluation at biochemical recurrence and assessment of metastatic disease. Importantly our findings demonstrate similar overall AJCC staging concordance in 92% of patients, with a few notable differences.

Significantly reduced urinary radiotracer excretion by [^{18}F]PSMA-1007 improves the characterisation of disease adjacent the bladder (prostate upstaging in 5/17 patients, and prostate bed upstaging in 3/33 patients) and ureters (regional nodal disease upstaging in three patients) compared to [^{68}Ga]Ga-PSMA-11. In one case a discrete bladder wall metastasis was also only identified with [^{18}F]PSMA-1007. In most cases this did not alter the overall stage of the disease because of additional identified sites of either nodal or distant metastases. However this information may still play an important role in pre-operative surgical planning, choice of treatment modality (radiotherapy may be preferred over exenterative surgery for T4 disease), guiding the extent of radiotherapy treatment (extension of local tumour volume delineation to cover adjacent infiltrated bladder, rectum and/or elective treatment of pelvic lymph nodes(21, 22), and the use of androgen deprivation therapy(23). These imaging findings are consistent with most literature, including a matched pair comparison of 240 scans with [^{18}F]PSMA-1007 vs F-DCFPyl identified suspected prostate/prostatic fossa lesions in a higher proportion of [^{18}F]PSMA-1007 scans, particularly for the indication of biochemical recurrence(24). Also in the setting of biochemical recurrence, [^{18}F]PSMA-1007 has previously been shown to be at least as accurate as [^{68}Ga]Ga-PSMA-11(14, 15, 25). [^{18}F]PSMA-1007 has also previously demonstrated accurate histopathologic correlation in eight patients for pelvic nodal disease in 18/19 pelvic nodes in eight patients, down to 1mm diameter(12). In contrast, a recent small pilot study by Ende et al. compared the performance of [^{68}Ga]Ga-PSMA-11 to [^{18}F]PSMA-1007 in biochemical recurrence in 12 patients following radical prostatectomy(26). In that study three lesions were identified in the prostate fossa on [^{68}Ga]Ga-PSMA-11 alone, compared with just one on [^{18}F]PSMA-1007.

There are other significant differences in physiologic tracer distribution, with all measured sites other than bladder demonstrating higher SUV on [^{18}F]PSMA-1007. In particular for nodal characterisation, uptake was consistently slightly higher on [^{18}F]PSMA-1007 than [^{68}Ga]Ga-PSMA-11 in sacral, coeliac and stellate ganglia and in benign inguinal nodes. Rauscher et al. previously raised concern about significantly increased number of benign lesions that could confound an inexperienced reader with ganglia and unspecific lymph nodes being most common. In our study, distant nodal assessment was concordant between both tracers in this series, precluding any misdiagnosis of coeliac or stellate ganglia. In the pelvis, nodal upstaging occurred in nodes adjacent to ureters in typical drainage pathways, with no additional lesions identified in a location attributable to presacral ganglia. Pathologic/concordantly avid nodal uptake was significantly higher on [^{18}F]PSMA-1007 than [^{68}Ga]Ga-PSMA-11 (SUVmax 11.1 vs 8.7, $p = 0.002$), potentially aiding accurate diagnosis.

Liver uptake is significantly higher with [^{18}F]PSMA-1007, contributing to the missed diagnosis of a solitary right adrenal metastasis adjacent similarly 'intense' liver activity. In clinical practice it is unlikely this would have been missed (it was previously reported on a clinical diagnostic CT and was prospectively identified by one reporter in the study) but nevertheless liver activity obscuring visceral metastases must be highlighted as a key potential pitfall of [^{18}F]PSMA-1007 PET/CT, as reported by others (27).

Our study identified six equivocal bone lesions that were not identified on [^{68}Ga]Ga-PSMA-11, one of which ([^{18}F]PSMA-1007 SUVmax 9.4) subsequently progressed and was confirmed a definite osseous metastasis. The remaining non-specific lesions ([^{18}F]PSMA-1007 SUVmax range 3.1-7.9) were either confirmed benign or no follow-up was available. Non-specific/equivocal bone lesions are a recognised issue in reporting of [^{18}F]PSMA-1007 PET/CT. Rauscher et al. reported that non-specific bone lesions were identified in 48% of 102 clinically matched patients imaged with [^{18}F]PSMA-1007 PET/CT, compared to 15% of 102 patients imaged with [^{68}Ga]Ga-PSMA-11 PET/CT(28). Further, a recent intraindividual comparison of [^{18}F]PSMA-1007 PET to one of three other prostate cancer PET tracers ([^{68}Ga]Ga-PSMA-11, [^{18}F]DCFPyL, and [^{18}F]JK-PSMA-7) identified 15 non-specific bone marrow foci on [^{18}F]PSMA-1007 PET that were not identified with other tracers, none of which demonstrated a morphological correlate on CT and post-contrast MRI(19). Our unpublished data (under review) identified non-specific bone lesions (NSBL) – defined as equivocal uptake in bone without an anatomic correlate on co-registered CT – in 94/214 (43.9%) of patients imaged with [^{18}F]PSMA-1007. In 77 of these patients with clinical follow-up (median 15.8 months), none met predefined criteria for a definite or likely bone metastasis. There was no statistical difference in clinical risk or PSA levels for patients with / without an isolated NSBL. When compared to a cohort of definite bone metastases, an SUVmax cut-point of <7.2 (in the absence of typical features on CT) maximised the sensitivity and specificity and is a proposed threshold to exclude bone metastasis. NSBL with SUVmax 7.2-11.1 may be classified as equivocal or metastatic, with patient clinical risk factors, scan appearance and potential management implications used to guide interpretation. Using this classification, 4/6 patients with NSBL would have been dismissed as benign (SUVmax 3.1-6.5), and two patients with NSBL would have remained equivocal (SUVmax 7.9 in left 5th rib, and SUVmax 9.4 in T11 vertebral endplate), with the latter most avid lesion being subsequently confirmed malignant during follow-up. By comparison, confirmed [^{18}F]PSMA-1007 avid bone metastases in our series demonstrated much higher uptake (median SUVmax 30.9 [IQR 20.8-41.5]).

A strength of our study is its prospective intraindividual study design, enabling definitive comparison of both [^{18}F]PSMA-1007 and [^{68}Ga]Ga-PSMA-11 uptake within the same lesions / patient. Most other studies evaluating [^{18}F]PSMA-1007 have been retrospective matched pair comparisons, retrospective single tracer or small pilot studies. Furthermore our blinded analysis by two independent nuclear medicine specialists (blinded to the other scan, reporter, and other imaging results), with use of an independent third reviewer in case of discordant staging, is a rigorous study design. Limitations of the study include the lack of a definitive gold standard, given the impracticality of taking a biopsy of every avid lesion. Concordant findings were considered true positive, but there is a limitation on evaluation of discordant findings beyond the results from available clinical follow-up.

Conclusion:

This large prospective intraindividual comparison of [^{18}F]PSMA-1007 PET/CT vs [^{68}Ga]Ga-PSMA-11 PET/CT has demonstrated overall high concordance (92%) for TNM stage in the context of prostate cancer primary staging, biochemical recurrence and evaluation of patients with metastatic disease. Reduced [^{18}F]PSMA-1007 urinary radiotracer excretion improves characterisation of disease adjacent the bladder (prostate or prostate bed following definitive treatment, including local invasion) and ureters (peri-ureteric nodes) compared to [^{68}Ga]Ga-PSMA-11. [^{18}F]PSMA-1007 demonstrates significantly higher uptake within involved nodes and bone metastases, and physiologic tissues including liver, spleen, neural ganglia, bone marrow and benign nodes. Inexperienced reporters of [^{18}F]PSMA-1007 PET should understand that hepatic uptake may obscure metastases within the liver or adjacent adrenal gland, and that [^{18}F]PSMA-1007 is associated with more equivocal bone lesions. Both tracers are acceptable for imaging of prostate cancer, with factors influencing choice including availability (local generator production of [^{68}Ga]Ga-PSMA-11 vs external cyclotron supply [^{18}F]PSMA-1007), preference for improved characterisation of disease in the prostate and pelvic nodes (favouring [^{18}F]PSMA-1007) versus likelihood of visceral metastasis (favouring [^{68}Ga]Ga-PSMA-11) and the experience of reporting specialists to exclude benign patterns of uptake, particularly neural ganglia and equivocal bone lesions.

Declarations:

Funding: No funding was received for conducting this study. Matthew J Roberts is supported by a Clinician Research Fellowship from the Metro North Office of Research, Queensland Health, and a Doctor in Training Research Scholarship from Avant Mutual Group Pty Ltd.

Conflicts of interest / Competing interests: The authors have no conflicts of interest to declare that are relevant to the content of this article.

Availability of data and material: Available upon reasonable request.

Code availability: not applicable.

Ethics approval and consent to participate: This trial was approved by the institutional review board of the Royal Brisbane and Women's Hospital Human Research Ethics Committee and was conducted in accordance with 1964 Helsinki Declaration. Written informed consent for participation and publication was provided.

Author contributions: All authors contributed to the study conception and design, or acquiring data, or analysing and interpreting data. Material preparation, data collection and analysis were performed by Maciej Debowski, Brooke Gulhane, Evyn Arnfield, David Pattison, Stuart Ramsay and Paul Thomas. The first draft of the manuscript was written by David Pattison and all authors commented on previous versions of the manuscript. All authors read and approved the final manuscript.

ACKNOWLEDGMENTS:

We would like to acknowledge the effort of nuclear medicine technologists, nursing and medical staff at Royal Brisbane and Women's Hospital and Q-TRaCE (QLD – The Radiopharmaceutical Centre of Excellence) radiochemistry staff who supported and contributed to the running of this trial, in addition to the enthusiastic participation of our patients. We are also grateful to Marita Prior for assistance with trial administration.

References:

1. Fitzmaurice C, Allen C, Barber RM, Barregard L, Bhutta ZA, Brenner H, et al. Global, Regional, and National Cancer Incidence, Mortality, Years of Life Lost, Years Lived With Disability, and Disability-Adjusted Life-years for 32 Cancer Groups, 1990 to 2015. JAMA Oncology. 2017;3(4):524.
2. Hupe MC, Philippi C, Roth D, Kümpers C, Ribbat-Idel J, Becker F, et al. Expression of Prostate-Specific Membrane Antigen (PSMA) on Biopsies Is an Independent Risk Stratifier of Prostate Cancer Patients at Time of Initial Diagnosis. Frontiers in Oncology. 2018;8.
3. Roberts MJ, Morton A, Donato P, Kyle S, Pattison DA, Thomas P, et al. (68)Ga-PSMA PET/CT tumour intensity pre-operatively predicts adverse pathological outcomes and progression-free survival in localised prostate cancer. Eur J Nucl Med Mol Imaging. 2021;48(2):477-82.
4. Hofman M, Lawrentschuk N, Francis R, Tang C, Vela I, Thomas P, et al. Prostate-specific membrane antigen PET-CT in patients with high-risk prostate cancer before curative-intent surgery or radiotherapy (proPSMA): a prospective, randomised, multicentre study. The Lancet. 2020;395(10231):1208-16.
5. Perera M, Papa N, Christidis D, Wetherell D, Hofman MS, Murphy DG, et al. Sensitivity, Specificity, and Predictors of Positive (68)Ga-Prostate-specific Membrane Antigen Positron Emission Tomography in Advanced Prostate Cancer: A Systematic Review and Meta-analysis. Eur Urol. 2016;70(6):926-37.
6. Hofman MS, Violet J, Hicks RJ, Ferdinandus J, Thang SP, Akhurst T, et al. [(177)Lu]-PSMA-617 radionuclide treatment in patients with metastatic castration-resistant prostate cancer (LuPSMA trial): a single-centre, single-arm, phase 2 study. Lancet Oncol. 2018;19(6):825-33.
7. Fendler WP, Calais J, Allen-Auerbach M, Bluemel C, Eberhardt N, Emmett L, et al. 68Ga-PSMA-11 PET/CT Interobserver Agreement for Prostate Cancer Assessments: An International Multicenter Prospective Study. Journal of Nuclear Medicine. 2017;58(10):1617-23.
8. Violet J, Jackson P, Ferdinandus J, Sandhu S, Akhurst T, Iravani A, et al. Dosimetry of 177Lu-PSMA-617 in Metastatic Castration-Resistant Prostate Cancer: Correlations Between Pretherapeutic Imaging and Whole-Body Tumor Dosimetry with Treatment Outcomes. Journal of Nuclear Medicine. 2019;60(4):517-23.
9. Iravani A, Hofman MS, Mulcahy T, Williams S, Murphy D, Parameswaran BK, et al. 68Ga PSMA-11 PET with CT urography protocol in the initial staging and biochemical relapse of prostate cancer. Cancer Imaging. 2017;17(1).
10. Heußer T, Mann P, Rank CM, Schäfer M, Dimitrakopoulou-Strauss A, Schlemmer HP, et al. Investigation of the halo-artifact in 68Ga-PSMA-11-PET/MRI. PLoS One. 2017;12(8):e0183329.
11. Bailey DL, Hofman MS, Forwood NJ, O'Keefe GJ, Scott AM, Van Wyngaardt WM, et al. Accuracy of Dose Calibrators for 68Ga PET Imaging: Unexpected Findings in a Multicenter Clinical Pretrial Assessment.

Journal of Nuclear Medicine. 2018;59(4):636-8.

12. Giesel FL, Hadaschik B, Cardinale J, Radtke J, Vinsensia M, Lehnert W, et al. F-18 labelled PSMA-1007: biodistribution, radiation dosimetry and histopathological validation of tumor lesions in prostate cancer patients. Eur J Nucl Med Mol Imaging. 2017;44(4):678-88.
13. Kesch C, Vinsensia M, Radtke JP, Schlemmer HP, Heller M, Ellert E, et al. Intraindividual Comparison of18F-PSMA-1007 PET/CT, Multiparametric MRI, and Radical Prostatectomy Specimens in Patients with Primary Prostate Cancer: A Retrospective, Proof-of-Concept Study. Journal of Nuclear Medicine. 2017;58(11):1805-10.
14. Giesel FL, Knorr K, Spohn F, Will L, Maurer T, Flechsig P, et al. Detection Efficacy of 18F-PSMA-1007 PET/CT in 251 Patients with Biochemical Recurrence of Prostate Cancer After Radical Prostatectomy. Journal of Nuclear Medicine. 2019;60(3):362-8.
15. Rahbar K, Afshar-Oromieh A, Seifert R, Wagner S, Schäfers M, Bögemann M, et al. Diagnostic performance of 18F-PSMA-1007 PET/CT in patients with biochemical recurrent prostate cancer. European Journal of Nuclear Medicine and Molecular Imaging. 2018;45(12):2055-61.
16. Giesel FL, Cardinale J, Schäfer M, Neels O, Benešová M, Mier W, et al. 18F-Labelled PSMA-1007 shows similarity in structure, biodistribution and tumour uptake to the theragnostic compound PSMA-617. European Journal of Nuclear Medicine and Molecular Imaging. 2016;43(10):1929-30.
17. Rauscher I, Krönke M, König M, Gafita A, Maurer T, Horn T, et al. Matched-Pair Comparison of 68Ga-PSMA-11 PET/CT and 18F-PSMA-1007 PET/CT: Frequency of Pitfalls and Detection Efficacy in Biochemical Recurrence After Radical Prostatectomy. Journal of Nuclear Medicine. 2020;61(1):51-7.
18. Kuten J, Fahoum I, Savin Z, Shamni O, Gitstein G, Hershkovitz D, et al. Head-to-Head Comparison of 68Ga-PSMA-11 with 18F-PSMA-1007 PET/CT in Staging Prostate Cancer Using Histopathology and Immunohistochemical Analysis as a Reference Standard. Journal of Nuclear Medicine. 2020;61(4):527-32.
19. Dietlein F, Kobe C, Hohberg M, Zlatopolskiy BD, Krapf P, Endepols H, et al. Intraindividual Comparison of 18F-PSMA-1007 with Renally Excreted PSMA Ligands for PSMA PET Imaging in Patients with Relapsed Prostate Cancer. Journal of Nuclear Medicine. 2020;61(5):729-34.
20. Amin MB, Edge S, Greene F, Byrd DR, Brookland RK, Washington MK, et al. AJCC cancer staging manual (8th edition). American Joint Commission on Cancer. New York: Springer International Publishing; 2017.
21. Yu JB, Makarov DV, Gross C. A new formula for prostate cancer lymph node risk. Int J Radiat Oncol Biol Phys. 2011;80(1):69-75.
22. Wang YJ, Huang CY, Hou WH, Wang CC, Lan KH, Chen CH, et al. The outcome and prognostic factors for lymph node recurrence after node-sparing definitive external beam radiotherapy for localized prostate cancer. World J Surg Oncol. 2015;13:312.
23. D'Amico AV, Chen MH, Renshaw A, Loffredo M, Kantoff PW. Long-term Follow-up of a Randomized Trial of Radiation With or Without Androgen Deprivation Therapy for Localized Prostate Cancer. Jama. 2015;314(12):1291-3.
24. Wondergem M, Van Der Zant FM, Broos WA, Knol RJ. Matched-pair comparison of 18F-DCFPyL PET/CT and 18F-PSMA-1007 PET/CT in 240 prostate cancer patients; inter-reader agreement and lesion

detection rate of suspected lesions. Journal of Nuclear Medicine. 2021:jnumed.120.2585.

25. Giesel FL, Will L, Kesch C, Freitag M, Kremer C, Merkle J, et al. Biochemical Recurrence of Prostate Cancer: Initial Results with [18F]PSMA-1007 PET/CT. Journal of Nuclear Medicine. 2018;59(4):632-5.
26. Ende J, Amin A, Sheehan-Dare G, Cusick T, Ho B, Keane J, et al. Pilot Trial Comparing the Performance of 68Ga-PSMA-11 PET/CT to 18F-PSMA-1008 PET/CT in the Detection of Prostate Cancer Recurrence in Men with Rising PSA Following Radical Prostatectomy. J Radiol Med Imaging. 2021;4(1):1039.
27. Hartrampf PE, Seitz AK, Krebs M, Buck AK, Lapa C. False-negative 18F-PSMA-1007 PET/CT in metastatic prostate cancer related to high physiologic liver uptake. European Journal of Nuclear Medicine and Molecular Imaging. 2020;47(8):2044-6.
28. Rauscher I, Krönke M, König M, Gafita A, Maurer T, Horn T, et al. Matched-Pair Comparison of 68Ga-PSMA-11 PET/CT and 18F-PSMA-1007 PET/CT: Frequency of Pitfalls and Detection Efficacy in Biochemical Recurrence After Radical Prostatectomy. Journal of Nuclear Medicine. 2020;61(1):51-7.

Tables

Table 1. Patient characteristics

Characteristic	Summary (n=50)
Age (years), mean (SD)	71.8 (6.7)
Scan indication, n (%)	
Staging	12 (24)
Restaging	27 (54)
Metastatic	11 (22)
Gleason, n (%)*	
6	1 (2)
7	20 (48)
8	10 (24)
9	11 (26)
PSA before PET/CT (ng/ml), median (IQR)	2.7 (0.7 – 12.0)
Scan indication PSA before PET/CT (ng/ml), median (IQR)	
Staging	12 (8.7 – 18)
Restaging	0.8 (0.5 – 2.6)
Metastatic	9.7 (0.5 – 98)
ISUP Grade group, n (%)*	
1	1 (2)
2	8 (19)
3	12 (29)
4	10 (24)
5	11 (26)
Androgen deprivation therapy at time of scan, n (%)	
No	36 (72)
Yes	14 (28)

**n=42; SD, standard deviation; IQR, interquartile range; ISUP, International Society of Urological Pathology.*

Table 2. Differences between [^{18}F]PSMA-1007 and [^{68}Ga]Ga-PSMA-11 for SUV in disease sites

Location	N	[^{18}F]PSMA-1007 Mean (SD)	[^{68}Ga]Ga-PSMA-11 Mean (SD)	Mean difference (95% CI)	P
SUVmax - disease					
Prostate primary tumour	17	20 (7.7 – 24.9)†	13.7 (7.6 – 29.4)†	-	0.056
Local recurrence	12	10.9 (7.0 – 20)†	7.6 (4.4 – 15.2)†	-	0.028
Nodal metastases	17	11.1 (7.7 – 17.6)†	8.7 (7.3 – 15.1)†	-	0.002
Bone metastases	13	30.9 (20.8 – 41.5)†	30.7 (18.5 – 39.3)†	-	0.016
Equivocal bone lesions	6	6.2 (5.3 – 7.9)†	2.4 (1.5 – 3)†	-	0.028
Adrenal metastasis	3	20.6 (8 – 40.4)‡	17.8 (9.8 – 36.2)‡	-	0.29
SUVmax - physiologic					
Parotid	50	25.5 (6.0)	17.8 (4.5)	7.7 (6.4 – 9.1)	<0.001
Stellate ganglia	50	3.2 (1.1)	2.2 (0.6)	1.0 (0.7 – 1.3)	<0.001
Coeliac ganglia	50	4.4 (1.9)	2.8 (1.3)	1.6 (1.2 – 2.1)	<0.001
Sacral ganglia	50	2.1 (0.7)	1.4 (0.5)	0.7 (0.5 – 0.9)	<0.001
Inguinal node	50	1.7 (0.6)	1.3 (0.4)	0.3 (0.2 – 0.4)	<0.001
SUVmean - physiologic					
Bone L2	50	1.5 (0.5)	0.8 (0.4)	0.7 (0.6 – 0.9)	<0.001
Liver	50	11.9 (2.9)	4.4 (1.3)	7.5 (6.9 – 8.2)	<0.001
Spleen*	50	11.6 (5.4)	7.1 (3.9)	4.5 (4.0 – 5.1)	<0.001
Bladder	50	3.0 (1.9 – 5.3)†	14.8 (10.3 – 19.7)†	-	<0.001

**Individual distributions skewed: Spleen [^{18}F]PSMA-1007 median (IQR) 10.3 (8.1 – 13.8) and [^{68}Ga]Ga-PSMA-11 median (IQR) 6.0 (4.9 – 8.1). Differences normally distributed.*

†median (IQR)

‡median (minimum – maximum)

Table 3a. T stage concordance

[^{18}F]PSMA-1007	[^{68}Ga]Ga-PSMA-11			
	T1/2	**T3a**	**T3b**	**T4**
T1/2	8			
T3a	1 (T3a)	1		
T3b	1 (T3a)		2	
T4	1 (T4)		2*	1

*Shading defines concordant scan findings; Brackets define consensus follow-up of discordant cases; * (1 case T4, 1 case N/A); N/A, no available follow-up.*

Table 3b. Local recurrence concordance

[^{18}F]PSMA-1007	[^{68}Ga]Ga-PSMA-11			
	Nil	**Equivocal**	**Local recurrence**	**Local recurrence & invasion**
Nil	20			
Equivocal				
Local recurrence	1 (N/A)	1 (Nil)	8	
Local recurrence & invasion			1(LRI)	2

Shading defines concordant scan findings; Brackets define consensus follow-up of discordant cases; N/A, no available follow-up; LRI, local recurrence & invasion

Table 3c. N stage concordance

[^{18}F]PSMA-1007	[^{68}Ga]Ga-PSMA-11		
	N0	**NE**	**N1**
N0	31		1 (N/A)
NE	1 (N0)		
N1	3*		14

*Shading defines concordant scan findings; Brackets define consensus follow-up of discordant cases; *(2 cases N1, 1 case N/A); N/A, no available follow-up*

Table 3d. M stage concordance

[^{18}F]PSMA-1007	[^{68}Ga]Ga-PSMA-11				
	M0	ME	M1a	M1b	M1c
M0	27				1 (M1c)
ME	6*				
M1a			3		
M1b				11	
M1c				1 (M1c)	1

*Shading defines concordant scan findings; Brackets define consensus follow-up of discordant cases; *(1 case M1, 5 cases M0)*

Table 3e. Overall AJCC prognostic stage concordance

[^{18}F]PSMA-1007	[^{68}Ga]Ga-PSMA-11								
	I	IIA	IIB	IIC	IIIA	IIIB	IIIC	IVA	IVB
I	2								
IIA									
IIB			5						
IIC				12				1 (N/A)	
IIIA					2				
IIIB						1			
IIIC							4		1 (IVB)
IVA				1 (IVA)		1 (IVA)		4	
IVB									16

Shading defines concordant scan findings; Brackets define consensus follow-up of discordant cases; N/A, no available follow-up

Supplementary Information

TABLE 1: Consensus resolution of discordant PET findings

Patient	[^{18}F]PSMA-1007				[^{68}Ga]Ga-PSMA-11				Follow-up	Consensus
	T	N	M	AJCC	T	N	M	AJCC		
T stage										
1	T3a	N0	M0	IIIC	T1/2	N0	M0	IIIC	Extracapsular extension on MRI	**T3a (F)**
2	T4	N1	M1b	IVB	T3b	N1	M1b	IVB	Nil definitive F/U investigation	**N/A**
3	T4	N1	M1b	IVB	T3b	N1	M1b	IVB	F/U [^{18}F]^{18}F-DCFPyL PET/CT: T4, clinically consistent with progression	**T4 (F)**
4	T4	N1	M1b	IVB	T1/2	N1	M1b	IVB	Cystoscopy & TURP: tumour invades trigone / bladder neck	**T4 (F)**
5	T3b	N0	M0	IIIC	T1/2	N0	M0	IIIC	Histopathology (prostatectomy): T3a; (note that MRI suggests T3b)	**T3a**
Local recurrence										
6	LR	N0	Me	IIIA	LRe	N0	M0	IIIA	F/U [^{18}F]PSMA-1007: Nil; (note LR unlikely given prior external RT & brachytherapy)	**Nil**
7	LRI	N1	M1b	IVB	LR	N1	M1b	IVB	Contrast CT: recurrent tumour direct invasion of vesicoureteric junction	**LRI (F)**
8	LR	N1	M0	IVA	Nil	N1	M0	IVA	Nil definitive F/U investigation	**N/A**
N stage										
9	LR	N0	M0	IIC	LR	N1	M0	IVA	Nil definitive F/U investigation	**N/A**
10	Nil	N1	M1a	IVB	Nil	N0	M1a	IVB	Nil definitive F/U investigation	**N/A**

11	Nil	Ne	M0	IIB	Nil	N0	M0	IIB	F/U [^{18}F]PSMA-1007: N0	**N0 (Ga)**
12	T3a	N1	M0	IVA	T3a	N0	M0	IIIB	F/U [^{18}F]PSMA-1007: N1, clinically consistent with progression	**N1 (F)**
13	Nil	N1	Me	IVA	Nil	N0	M0	IIC	F/U [^{18}F]^{18}F-DCFPyL: N1, clinically consistent with progression	**N1 (F)**
M stage - Bone										
6	LR	N0	Me	IIIA	LRe	N0	M0	IIIA	F/U [^{18}F]PSMA-1007: M1b, clinically consistent with progression	**M1b**
13	Nil	N1	Me	IVA	Nil	N0	M0	IIC	F/U [^{18}F]^{18}F-DCFPyL: M0	**M0 (Ga)**
14	T1/2	N1	Me	IVA	T1/2	N1	M0	IVA	F/U PSA <0.01 after definitive local therapy	**M0 (Ga)**
15	LR	N0	Me	IIC	LR	N0	M0	IIC	F/U [^{18}F]PSMA-1007: unchanged lesion after 20 months; PSA decline 1.3 to 0.02 with salvage external RT	**M0 (Ga)**
16	Nil	N0	Me	IIB	Nil	N0	M0	IIB	F/U [^{18}F]^{18}F-DCFPyL: M0	**M0 (Ga)**
17	LR	N0	Me	IIIC	LR	N0	M0	IIIC	F/U diagnostic CT & bone scan: M0	**M0 (Ga)**
M stage - Visceral										
18	LRI	N1	M1c	IVB	LRI	N1	M1b	IVB	F/U diagnostic CT: M1c	**M1c (F)**
19	Nil	N0	M0	IIIC	Nil	N0	M1c	IVB	Histopathology: M1c	**M1c (Ga)**

AJCC, AJCC prognostic stage group; F/U, follow-up; N/A, not available; TURP, transurethral resection of the prostate; RT, radiotherapy; (F), consistent with [^{18}F]PSMA-1007; (Ga), consistent with [^{68}Ga]Ga-PSMA-11; RT,

radiotherapy; LR, local recurrence; LRe, local recurrence-equivocal; LRI, local recurrence with invasion adjacent organs; Nil, nil local recurrence; Ne, Nodes equivocal; Me, equivocal bone metastasis

Figures

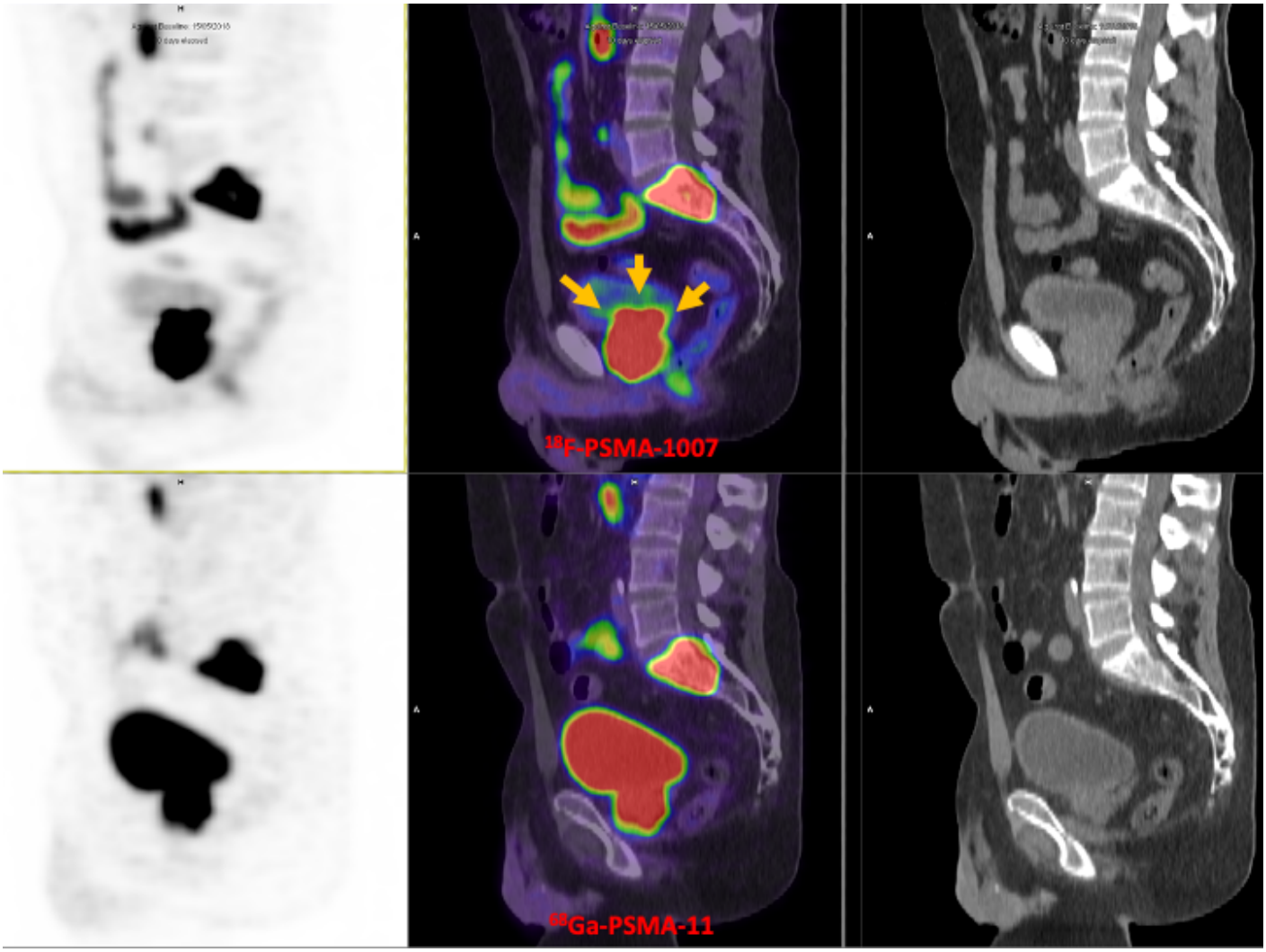

Figure 1

[18F]PSMA-1007 clearly identifies bladder invasion (T4, orange arrows), not visible on [68Ga]Ga-PSMA-11 due to intense urinary radiotracer excretion. Images left to right, sagittal PET, sagittal fused PET/CT and sagittal CT; SUV window threshold 0-10.

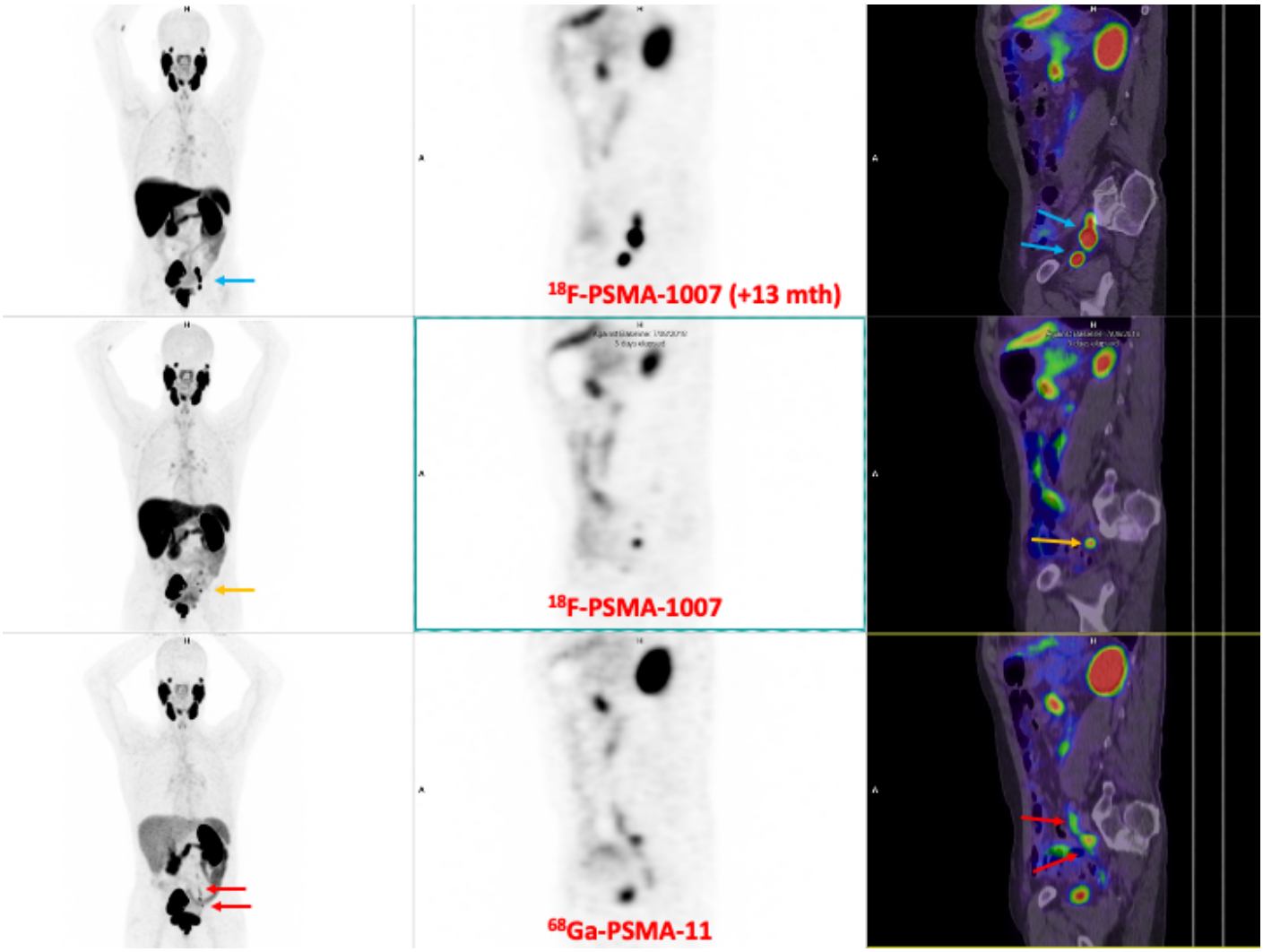

Figure 2

[18F]PSMA-1007 identified two discrete pelvic side wall nodes adjacent to surgical clips (orange arrows), which were considered pooling of urinary radiotracer on [68Ga]Ga-PSMA-11 (red arrows). Followup [18F]PSMA-1007 performed 13 months later confirmed definite progressive nodal disease at this site (blue arrows). Images left to right, maximum intensity projection, sagittal PET and sagittal fused PET/CT images; SUV window threshold 0-10.

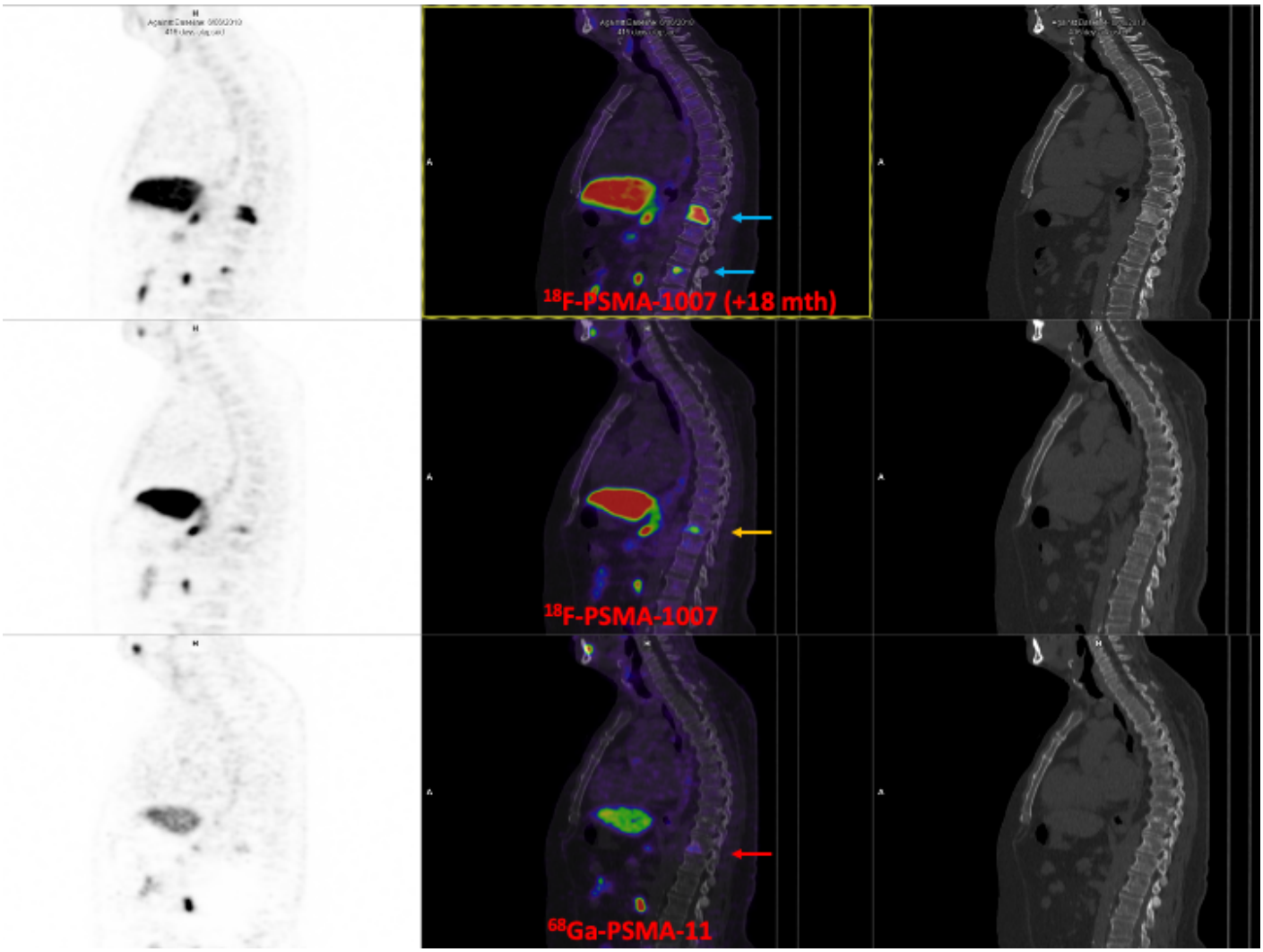

Figure 3

[18F]PSMA-1007 demonstrated focal uptake at the inferior endplate of T11 vertebra associated with sclerosis (orange arrows), considered equivocal given the atypical appearance of this solitary lesion. There was no significant uptake at this site on [68Ga]Ga-PSMA-11PET/CT (red arrows). Subsequent followup [18F]PSMA-1007 PET/CT confirmed increasing uptake and sclerosis at this site, and additional FPSMA avid osseous lesions consistent with progressive metastatic disease (blue arrows). Images left to right, sagittal PET, sagittal fused PET/CT and sagittal CT; SUV window threshold 0-10.

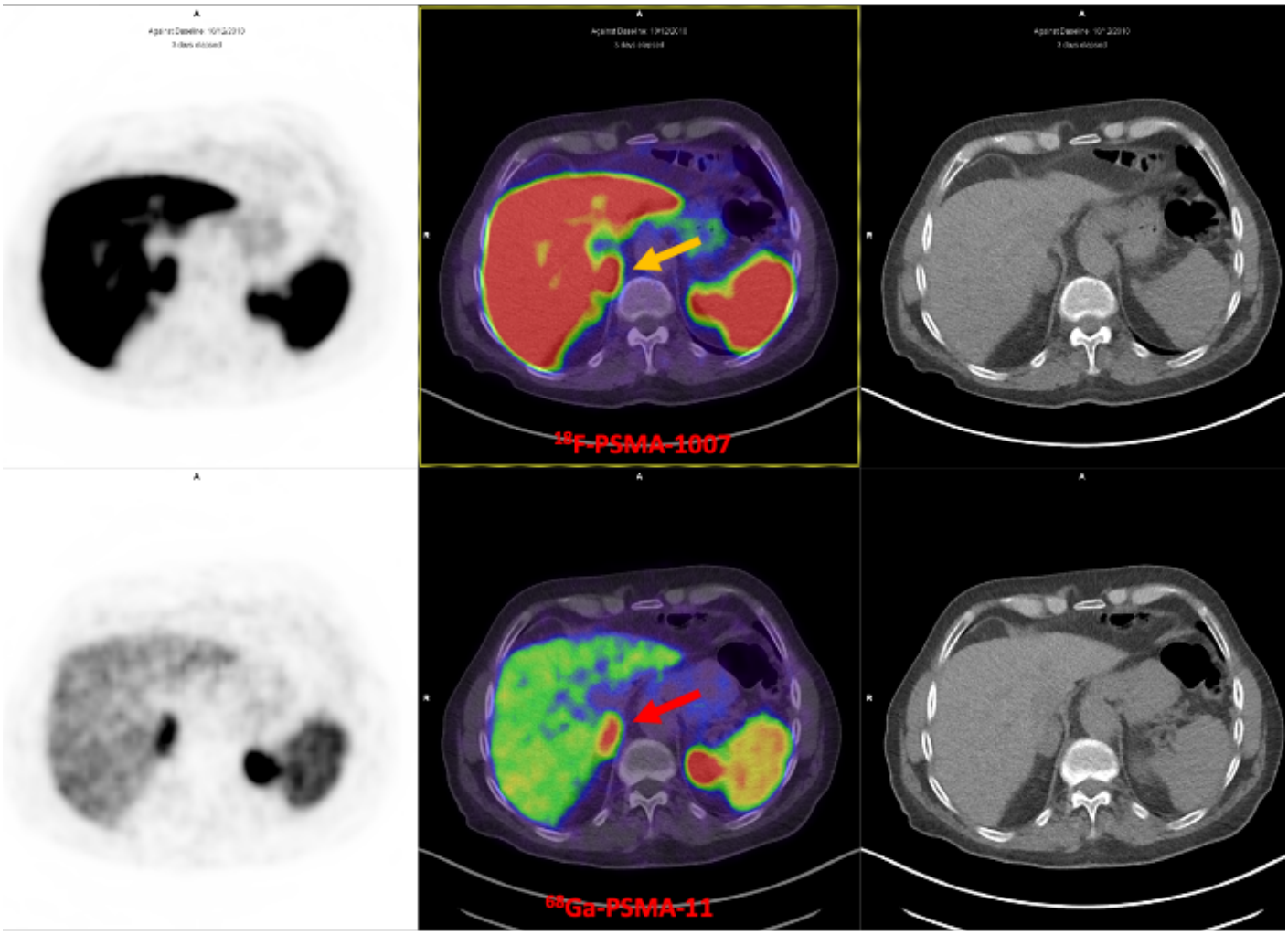

Figure 4

[18F]PSMA-1007 clearly identifies a discrete separate focus of bladder uptake consistent with visceral metastasis (M1c, orange arrow), not visible on [68Ga]Ga-PSMA-11 due to intense urinary radiotracer excretion. Images left to right, axial PET, axial fused PET/CT and axial CT; SUV window threshold 0-10.

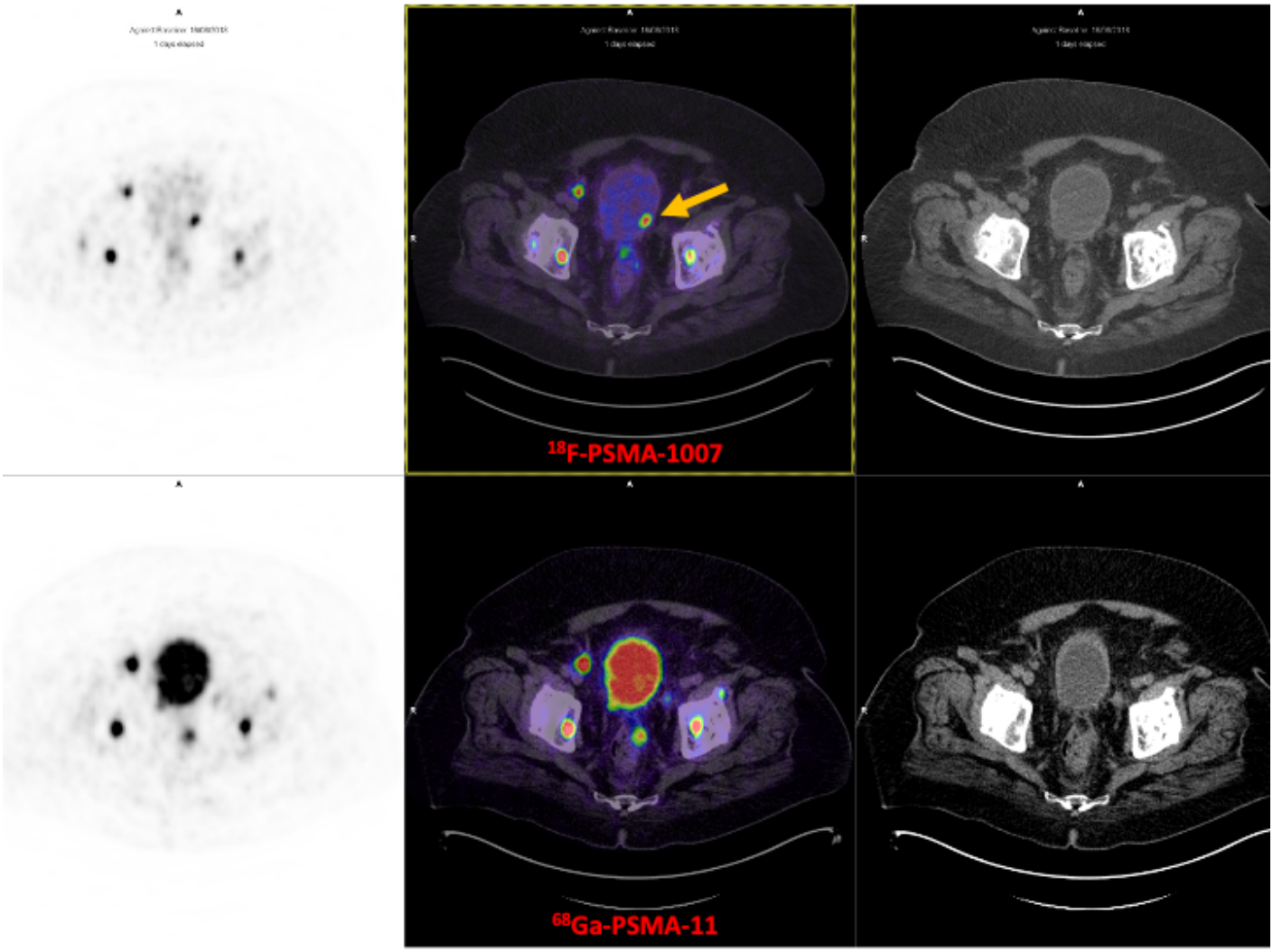

Figure 5

Intensely [18F]PSMA-1007 avid right adrenal metastasis (orange arrow) was not identified due to similarly intense physiologic uptake in the adjacent liver. This lesion was prospective identified on [68Ga]Ga-PSMA-11 PET/CT (red arrow), and subsequently histopathologically confirmed as metastatic prostate carcinoma. Images left to right, axial PET, axial fused PET/CT and axial CT; SUV window threshold 0-10.